

Practical control method for ultra-precision positioning using a ballscrew mechanism

Guilherme Jorge Maeda, Kaiji Sato*

Interdisciplinary Graduate School of Science and Engineering, Tokyo Institute of Technology, 4259 Nagatsuta, Midori-ku, Yokohama 226-8502, Japan

Received 7 March 2007; received in revised form 18 September 2007; accepted 26 October 2007

Available online 24 November 2007

Abstract

This paper describes a practical control method for nanometer level point-to-point positioning (PTP) using a conventional ballscrew mechanism. A nominal characteristic trajectory following controller (NCTF controller) is used for the ultra-precision positioning. The controller design, which is comprised of a nominal characteristic trajectory (NCT) and a PI compensator, is free from exact modeling and parameter identification. The NCT is determined from an open-loop experiment and the PI compensator is used to make the mechanism motion to follow the NCT. The compensator gain values are restricted by the practical stability limit of the control system, which is easy to determine. Using a high integral gain causes excessive overshoot, so an antiwindup integrator is used to improve the system performance. The NCTF control system achieves a positioning resolution of 5 nm and is robust against friction variations.

© 2007 Elsevier Inc. All rights reserved.

Keywords: Nanopositioning; Ultra-precision positioning; Point-to-point; Friction; Ballscrew; Antiwindup

1. Introduction

Precision positioning systems that can achieve an accuracy on the order of micrometers or nanometers are essential in the optical, semiconductor, and nanotechnology industry. These positioning systems usually have one or more elements that introduce friction, like motors with brushes and/or bearings with mechanical contact. Friction is well known to cause steady-state and tracking errors, to limit cycles and to slow the motion of the mechanism. Thus, it is important to consider friction compensation in controller design. However, controller design of mechanisms with friction tends to be difficult because: (1) characteristics of mechanisms with friction are nonlinear, thus simple controllers like PID controllers do not offer the best possible performance and (2) friction compensation usually requires the identification of friction characteristics, which can vary.

In order to compensate for friction, efforts have been made to understand the effects of friction on control performance [1] and its dynamics [2,3]. Control systems for precision/ultra-

precision positioning must compensate for friction on the micro-scale, which requires an understanding of the nonlinear behavior of the mechanism before the breakaway torque is achieved [4–6]. Nevertheless, friction parameters, especially in the microdynamic regime, tend to change with time and position [7,8] and seem to behave stochastically [5], making them difficult to predict exactly. Also, a complete model for macro-microdynamics has to address the transition between the two dynamics [9]. The inclusion of the friction dynamics as part of the control law does improve precision positioning [8,10–12], but the controller design becomes time consuming and difficult.

In this research, a conventional ballscrew mechanism is used as the friction mechanism. Although some studies have achieved nanometric accuracy with a ballscrew system (e.g. [11–14]), this research differs significantly in the ease of design and control structure. The controller used, called the NCTF controller has a simple structure and its design method does not require exact parameter identification, which makes it easy to design, understand, and adjust.

The NCTF control system has previously been used for different mechanisms, then evaluated and compared with other types of practical controllers. The influence of the NCTF controller parameters and actuator saturation were discussed for a

* Corresponding author. Tel.: +81 45 924 5045; fax: +81 45 924 5483.
E-mail address: kaiji@pms.titech.ac.jp (K. Sato).

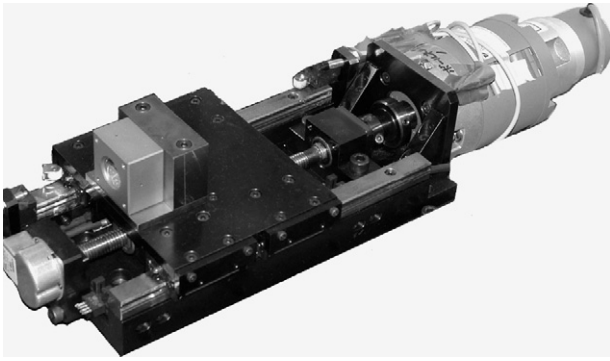


Fig. 1. Ballscrew mechanism used in this research.

rotary mechanism in [15]. In [16,17], performance improvement by means of an antiwindup integrator was presented. The performance of the NCTF controller was then compared to those delivered by conventional PID's [15,18]. The NCTF controller performance was also compared to two other practical controllers that address friction compensation: a PD controller with a nonlinear proportional feedback compensator, and a PD controller with a smooth nonlinear feedback compensator [19,20]. Sato et al. [21] designed and compared the performance of the NCTF controller with that of a PID controller using a linear motor mechanism. In this study, the mechanism was driven by a voice coil motor and had an adjustable-preload linear ball guide. A positioning accuracy of better than 50 nm was achieved.

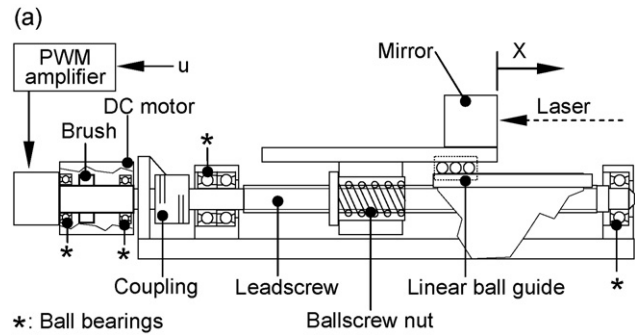
The purpose of this research is to clarify the NCTF control method for a ballscrew mechanism used in ultra-precision positioning. Mechanically, the ballscrew mechanism is more complex than the rotary and the linear motor mechanism mentioned above. Regardless of the mechanical complexity, the control design method should still be easy and straightforward. The positioning accuracy and resolution are expected to be better than 10 nm.

This paper is organized as follows. The experimental setup is introduced in Section 2. In Section 3, the NCTF controller design is explained, including the derivation of the design parameters and analyses of the linear and the practical stability limit. Section 4 details the performance improvement by means of an antiwindup integrator. In Section 5, the performance of the control system is evaluated by experiment and simulation. Finally, Section 6 discusses the feasibility of NCTF controller design method for mechanisms with a large range of friction variation (including a pure inertia mechanism) and different NCT inclinations.

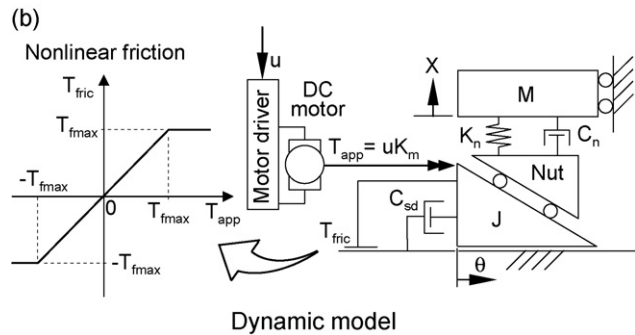
2. Experimental setup

Fig. 1 shows a picture of the ballscrew mechanism, which is the controlled mechanism in this study and Fig. 2 details the structure and dynamic model of the mechanism.

The mechanism has several sources of friction: the dc motor, the preloaded double-nut, the linear ball guides, and the ball bearings supporting the screw shaft. The overall combination



Structure of the mechanism



Dynamic model

Fig. 2. Structure and dynamic model of the mechanism.

of nonlinear friction effects are modeled as the frictional torque T_{fric} in Fig. 2(b). The stiffness of the connection between the screw and nut is represented as the spring constant K_n . The vibration between the screw and nut is damped by a damper having coefficient C_n . Table 1 shows the description and values of the model parameters. Values of T_{fmax} and C_{sd} tend to vary and depend on the warm-up condition. The simulated responses in Figs. 13 and 14 are calculated using their adjusted values.

As additional information of interest, the PWM power amplifier (Copley: 4122Z) is limited at 45V/6 A and the dc motor (Yaskawa: UGTMEM-06LB40E) has a back EMF constant of 0.086 Vs/rad. The controller sampling frequency is 5 kHz and its feedback position is determined by a laser position sensor with resolution of 1.24 nm (Agilent: 10897B). The lead of the ballscrew is 2 mm/rev and the maximum travel range of the table is 55 mm.

Table 1
Model parameters

Symbol	Description	Value
K_m	Torque constant of the motor	0.172 Nm/A
M	Table mass	3.57 kg
J	Moment of inertia of the rotary parts	1.81×10^{-4} kg m ²
T_{fric}	Nonlinear friction	–
T_{app}	Applied torque to the ballscrew	–
T_{fmax}	Coulomb friction	0.046 Nm ^a
C_{sd}	Viscous friction	0.00097 Nms/rad ^a
K_n	Spring constant (screw/nut)	8.3×10^5 N/m
C_n	Damping coefficient (screw/nut)	1700 Ns/m

^a May vary according to the warm-up condition.

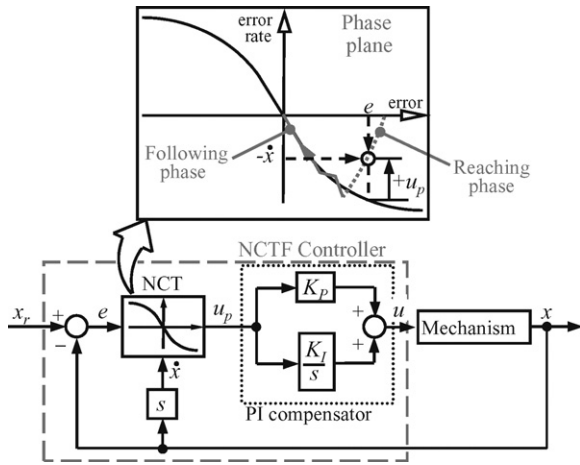


Fig. 3. Structure of the NCTF control system.

3. NCTF control concept and its previous controller design for mechanisms with friction

3.1. Concept

Fig. 3 shows the structure of the NCTF control system. The controller is composed of a nominal characteristic trajectory (NCT) and a PI compensator. The objective of the PI compensator is to make the mechanism motion follow the NCT, finishing at the origin of the phase-plane. The output of the NCT is a signal u_p , which is the difference between the actual error rate of the mechanism ($-\dot{x}$) and the error rate of the NCT. On the phase-plane, the table motion is divided into a reaching phase and a following phase. During the reaching phase, the compensator controls the table motion to achieve the NCT. The next step is the following phase, where the PI compensator causes the mechanism motion to follow the NCT, leading it back to the origin of the phase-plane.

The NCT is constructed from the actual response of the mechanism influenced by the friction and saturation effects. Thus the PI compensator tuned necessarily has the ability to make the mechanism motion follow the NCT macroscopically. The PI compensator works for reduction of the difference between the NCT and the actual motion when disturbance forces and mechanism characteristic changes increase the difference.

In a large working range where the saturation characteristic influences the mechanism motion, the reduction of the difference between them is desired so that the mechanism reaches the reference quickly without significant overshoot. However in a small working range, the elimination of static deviation is more important than the reduction of the difference. As shown in Fig. 4, the NCTF controller can be expressed using a variable PI element and a PD element. The NCT works as a variable gain element. The variable PI element has larger gain as the error decreases. The gain maximizes near the origin on the phase-plane, that is, near the reference position. This characteristic is useful to quickly eliminate the static deviation caused by the friction. The characteristic also tends to reduce the vibration and the overshoot [21].

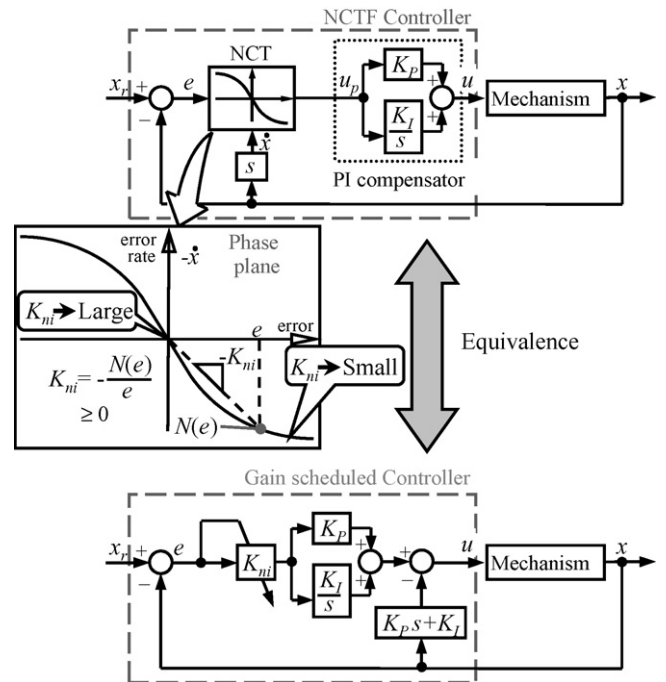


Fig. 4. Expression of the NCTF control system.

3.2. Design procedure

The theoretical discussion and the previous NCTF control design method is detailed in [15,21]. The design of the NCTF controller is comprised of three steps:

- (i) The mechanism is driven with an open-loop step input while its displacement and velocity are measured. Fig. 5(a) shows the open-loop response of the ballscrew mechanism.
- (ii) The NCT is constructed on the phase-plane using the displacement and velocity of the mechanism during the deceleration. Fig. 5(b) shows the NCT constructed from the open-loop experiment. In this figure, the trajectory from the response includes a circling motion caused by a spring-like behavior. This circling motion has negative effects on positioning and should be eliminated [21,22]. In order to do so, the NCT is linearized with a straight line close to the origin.
- (iii) The PI compensator is designed using the open-loop response and the NCT information. The PI gains are chosen within the stable operation region which can be previously calculated independently of the actual mechanism characteristic.

The derivation of the NCTF controller parameters are based on a linear macrodynamic model expressed as

$$\frac{X}{U} = K \frac{\alpha}{s(s + \alpha)} \quad (1)$$

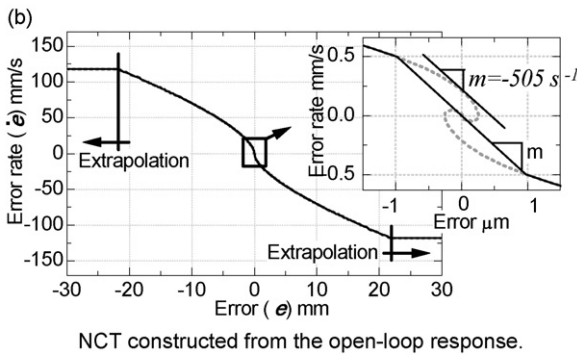
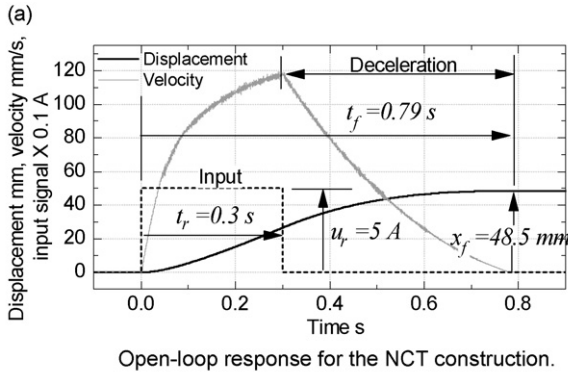


Fig. 5. Open-loop response and construction of the NCT.

When the value of u is constant with amplitude u_r , and zero after t_r (see Fig. 4(a)), parameter K becomes

$$x_f = Ku_r t_r \rightarrow K = \frac{x_f}{u_r t_r} \quad (2)$$

Fig. 6 shows the block diagram of the continuous closed-loop NCTF control system with the simplified object model near the NCT origin (where the NCT is linear and has an inclination $\alpha = -m$). The proportional and integral compensator gains are calculated from

$$K_P = \frac{2\zeta\omega_n}{\alpha K} \quad (3a)$$

$$K_I = \frac{\omega_n^2}{\alpha K} \quad (3b)$$

When choosing ζ and ω_n , the designer must consider the stability of the control system. Regarding the digital system, a linear stability analysis is carried out with the sampled-data system shown in Fig. 7. Applying the Jury's test ([23], p. 35), a numerical plot of the stability limit is shown in Fig. 8. The linear stability limit can be calculated independently of the actual mechanism characteristic. The limit also has negligible variations on the αT axis.

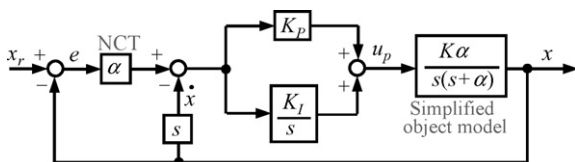


Fig. 6. NCTF control system with the simplified object model.

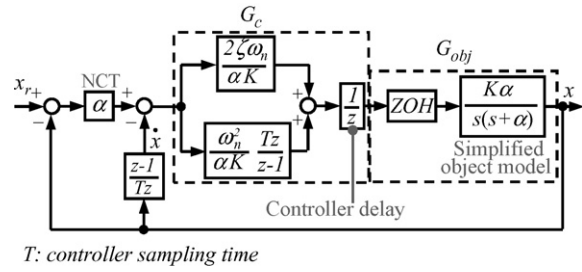


Fig. 7. Sampled-data system used for a linear stability analysis.

However the stability limit is too limited. Coulomb friction neglected in Fig. 7 is known to increase the stability of the system [1], allowing for the use of higher gains than those predicted by a linear analysis. The higher gains are expected to produce higher positioning performance. Thus the practical stability limit is necessary for selecting the higher gains in step (iii) of the design procedure.

4. Practical stability limit and choice of the design parameters

4.1. Decision of practical stability limit

This section introduces a simple method to find the practical stability limit of the NCTF control system. From Fig. 8 it is observed that the integral element has a negligible influence on the stability of the linear system. For the following analysis, it will also be assumed that the integral element has a negligible influence on the stability of the actual system. Experiments and simulations will show that this assumption is valid.

The practical stability limit is found by driving the mechanism with the NCTF controller using only the proportional element. The value of the proportional gain is increased until continuous oscillations are generated. The determined proportional gain is called K_{Pu} (2.4 As/mm in the case of the ballscrew mechanism), which represents the actual ultimate proportional gain. Using Eq. (3a), the practical stability limit ζ_{prac} is given as

$$\zeta_{prac} = K_{Pu} \left(\frac{\alpha K}{2\omega_n} \right) \quad (4)$$

Eq. (4) represents the maximum values allowed for a given ζ , before the control system becomes unstable. In the case of the ballscrew mechanism, Eq. (4) becomes

$$\zeta_{prac} = 2.4 \left(\frac{505 \times 32.3}{2\omega_n} \right) \quad (5)$$

In order to prove the suitability of ζ_{prac} , the NCTF controller (using the proportional and integral elements), is designed as follows: for a fixed value of $\omega_n T_k$ (where $k = 1, \dots, 7$), the compensator gains are calculated from Eqs. (3a) and (3b). The parameter ζ_k is increased until the system achieves instability. The points defined by ζ_k and $\omega_n T_k$ are plotted in Fig. 9. The procedure performed both experimentally and by simulations using the mechanism model in Fig. 2(b). As the results show, ζ_{prac} fits closely to all the points representing the NCTF control stability

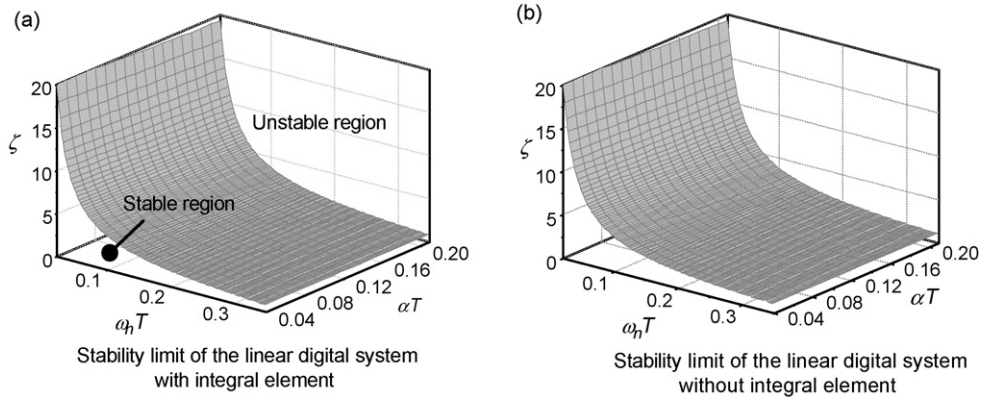


Fig. 8. Linear stability limit of the linear digital system by the Jury's test.

limit. In addition, it is observed that ζ_k represented by the linear stability limit curve is much smaller than the ζ determined by the practical stability limit.

4.2. Choice of the design parameters ω_n and ζ

Fig. 10 depicts three different compensators A, B and C and their respective gains. The three compensators are chosen to have 40% of the values of ζ_{prac} calculated from Eq. (5), so that the margin of safety of the design is 60%.

Fig. 11 shows that the positioning resolution improves as $\omega_n T$ increases. Since compensator C produces the best performance, it is chosen as the final controller for performance evaluation.

During the design parameter selection, the designer may be tempted to use large values of $\omega_n T$ in order to improve the performance. However, it is observed from Eqs. (3a) and (3b) that as $\omega_n T$ increases, K_I increases exponentially while K_P is kept constant. Excessively large values of $\omega_n T$ will cause the controller to behave as a pure integral controller, which may lead to instability. Therefore, the choice of $\omega_n T$ should start with small values and progress to large ones, but never the opposite. It should be noted that this procedure can be completed without any previous information about the model parameters.

The use of high integral gain is a key factor for improving positioning resolution. However, the integral gain also causes an undesirable overshoot during step input responses because of

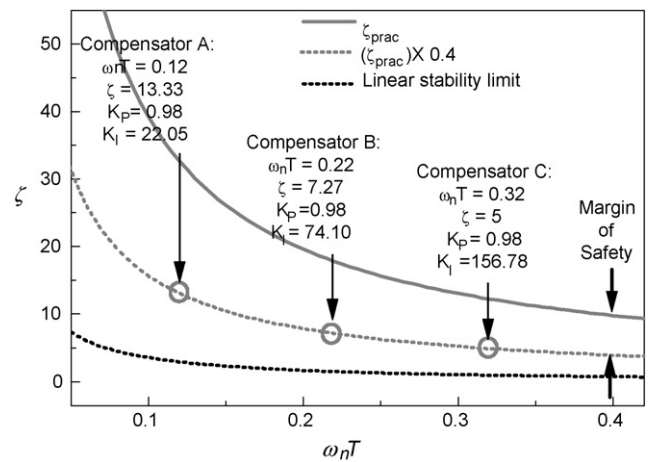


Fig. 10. Three different compensators respecting a margin of safety of 60%.

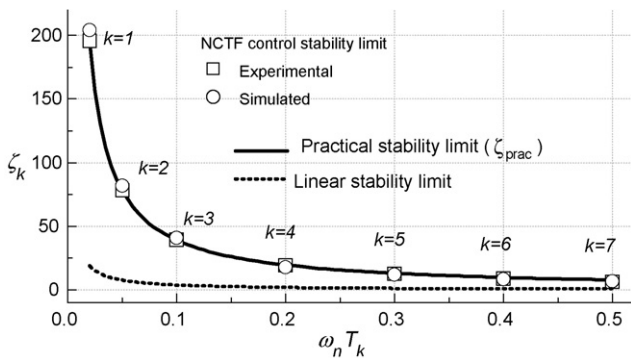


Fig. 9. Practical stability limit (ζ_{prac}) compared to experimental and simulated results.

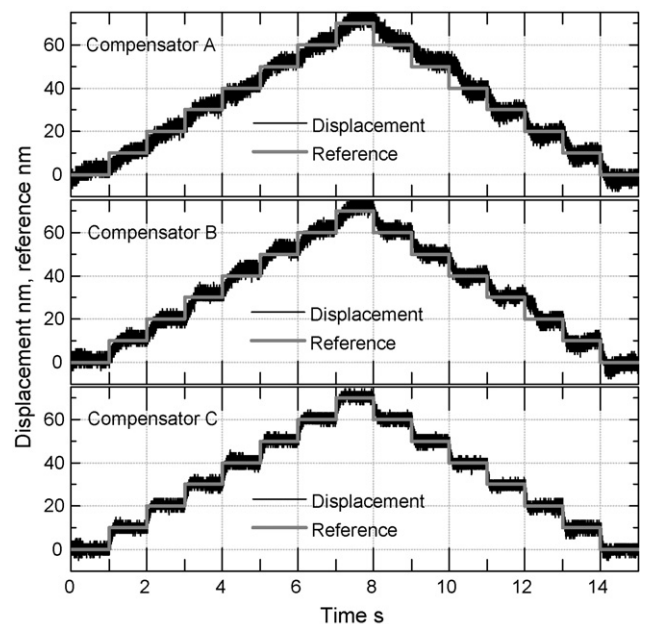


Fig. 11. Response of the compensators A, B, and C for a 10 nm stepwise input.

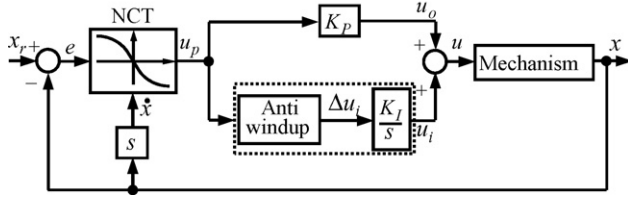


Fig. 12. NCTF controller structure with the conditionally freeze antiwindup.

the integrator windup effect. Thus, antiwindup integrators are useful for performance improvement.

Up until now, antiwindup integrators with the NCTF controller have been applied to a rotary positioning system: a tracking antiwindup [16] and a conditionally freeze integrator [17]. Both methods were shown to improve robustness. Although the tracking antiwindup method has only one design parameter, there are no clear rules on how to determine a proper parameter value, except for rules of thumb. The conditionally freeze integrator rule requires only a maximum control output signal as a design parameter, which is easy to determine.

Due to the ease of implementation, this research employs the conditionally freeze integrator [17]. The antiwindup element controls the input of the integrator, as shown in Fig. 12, with the following rule:

$$\Delta u_i = \begin{cases} 0, & |u_o + u_i| > u_s \text{ and } e \cdot u_i \geq 0 \\ e, & \text{otherwise} \end{cases} \quad (6)$$

where u_o is the proportional control signal, u_i is the integrated control signal, Δu_i is the change rate of u_i , and u_s is the maximum value of the control signal.

The maximum output control signal of the ballscrew mechanism, which defines the saturation of the actuator, is 6 A. The effect of the antiwindup on positioning performance is shown in Fig. 13, where compensator C is used in the NCTF controller. For a step input of 20 mm, the overshoot was reduced from 9.3%

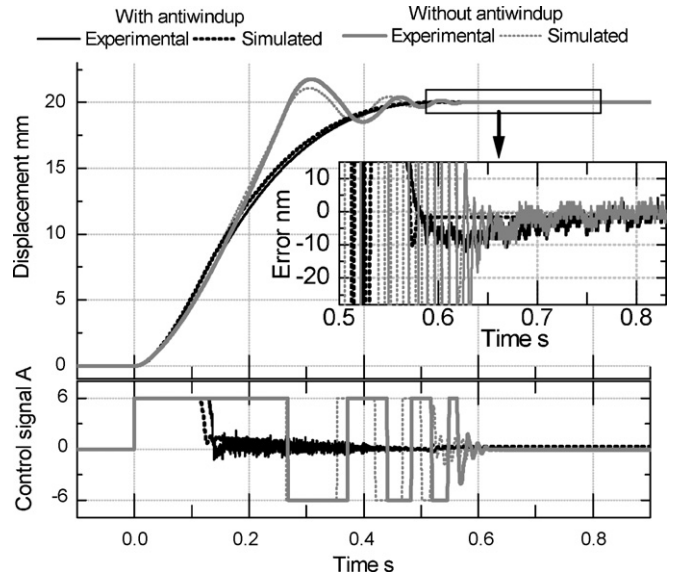


Fig. 13. Improvement of the performance with the antiwindup.

to less than 0.01%. Furthermore, the positioning time needed to reduce the error to less than 10 nm did not change. The control signal plot shows that the antiwindup better utilizes the driving force, saturating only during the reaching phase.

5. Performance evaluation

In this section, the PTP positioning performance of the NCTF controller with the ballscrew mechanism is evaluated. The parameters of the compensator are given in Fig. 10 using compensator C. The controller also includes the conditionally freeze integrator.

Fig. 14 shows the positioning performance for a small step of 10 μm and a large step input of 20 mm. The NCT works as a non-linear gain element as shown in Fig. 4. Its gain decreases when

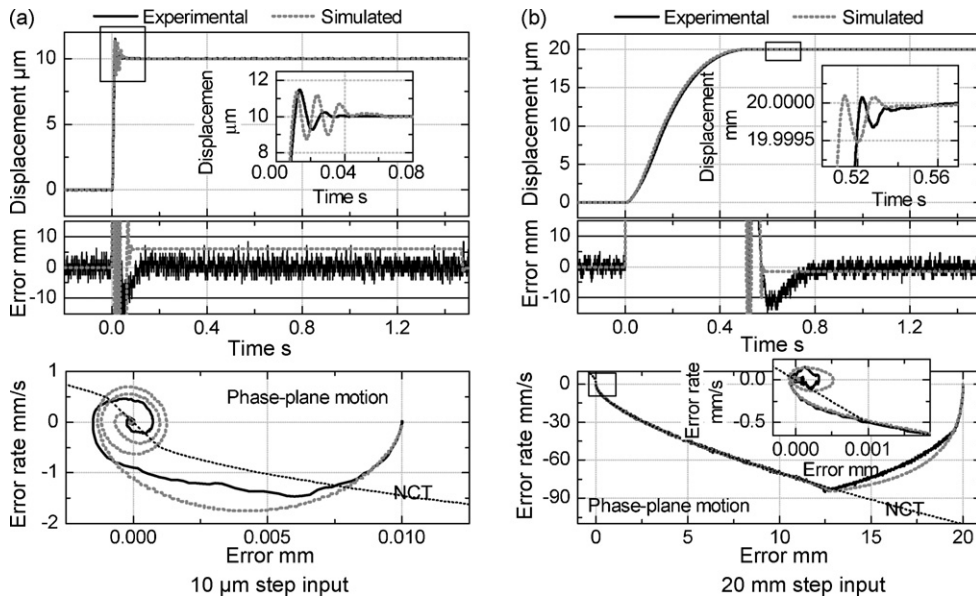
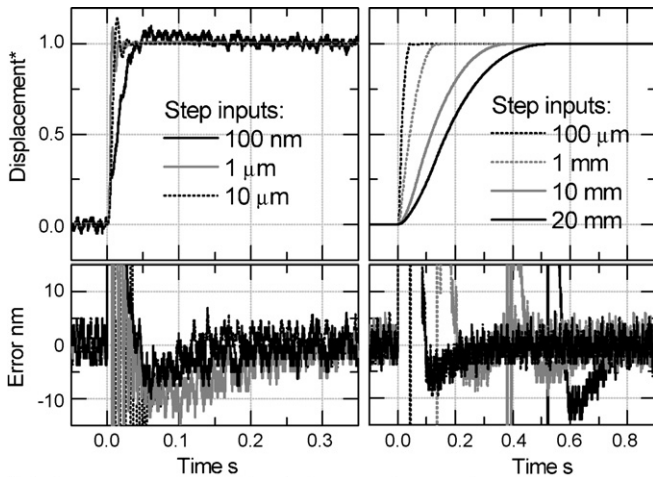


Fig. 14. Response to 10 μm and 20 mm step inputs.



*Displacements normalized to their respective step input heights

Fig. 15. Response to several step input heights.

the error becomes larger. Thus, the higher step input increases the rise time. However, in spite of the difference in step input heights, both cases achieve a positioning accuracy of less than 10 nm. The simulated results agree relatively well with the experimental ones.

Fig. 15 shows the PTP performance for step inputs of 100 nm, 1 μm , 10 μm , 100 μm , 1 mm, 10 mm, and 20 mm. The figures at the top show the displacements normalized by their respective step input heights. The lower figures show their respective errors (actual values, not normalized), proving that positioning accuracy is better than 10 nm, independent of the step height.

Fig. 16(a) details the positioning resolution of the control system. Stepwise inputs of 5 nm are used as reference, and the experiment is repeated for two different frictional conditions: before and after warming up. The warm-up condition is achieved by driving the mechanism with a sinusoidal reference of 20 mm in amplitude at a frequency of 0.6 Hz over 40 s. After the warm-up, the Coulomb friction and viscous friction were reduced by 13% and 24%, respectively. In spite of the changes in friction, a positioning resolution of 5 nm is still maintained, proving that the designed NCTF controller is robust against friction variations. Fig. 16(b) shows the sensor output under the open-loop condition. The input signal to the motor is zero and the amplitude of the measurement noise is the same as the positioning resolution achieved by the NCTF control system. Thus, the achieved positioning performance of the control system is on the limit of the measurement resolution.

6. Extension of the NCTF controller design method

The purpose of this section is to examine the applicability of the NCTF controller design method – the procedure for determining the controller parameters – to cases different from the ballscrew mechanism case described in Section 4. As a first case, an approximately pure inertia mechanism, which is a characteristic of friction free mechanisms, is considered. In the second case, a mechanism with large variation of Coulomb friction is evaluated. In the third case, different inclinations of the NCT are

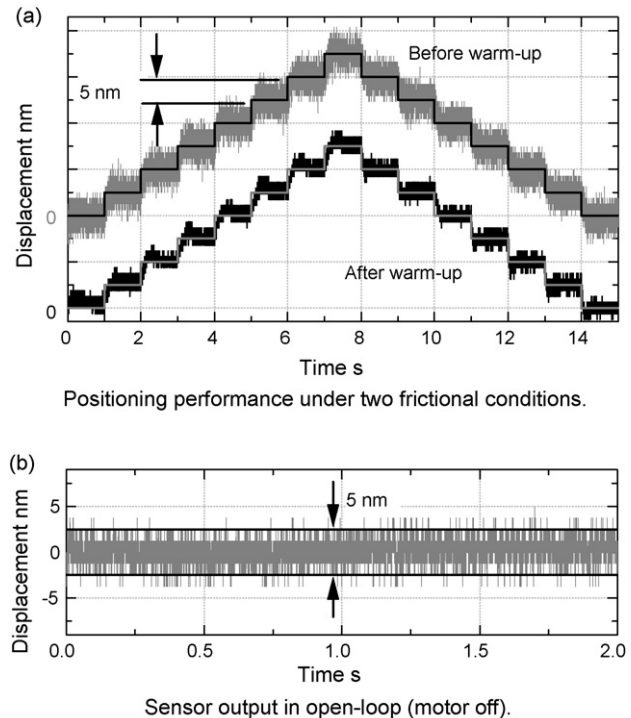


Fig. 16. Positioning resolution and sensor output (motor off) with same amplitudes.

considered, which is useful if the designer wants to modify the NCT close to the origin.

The controller design procedure is the same as the one used for the actual ballscrew mechanism for all three cases. The procedure involves constructing the NCT from an open-loop experiment and determining parameters α and K . The practical stability limit is found by driving the mechanism with the proportional controller. The NCTF control stability limit is obtained by fixing a value of $\omega_n T$ and increasing ζ until instability is reached with the compensator using the proportional and integral elements. The practical stability limit and the NCTF control stability limit are then compared. A close approximation of both stability limits proves that the design procedure is applicable.

For the first and second cases, the analyses are based on simulated results, since they are related to large variations in friction parameters that are impossible to achieve with a real mechanism. In the third case, the analysis is based on experimental results.

6.1. Case 1: practical stability limit under different damping conditions

The system depicted in Fig. 17 is used for the simulations. This system allows for the investigation of the effects of damping variations. The object does not include nonlinear friction and subscripts “c” and “obj” refer to the controller and object (mechanism) parameters, respectively. Parameters α_c and K are the same as those used with the actual ballscrew mechanism ($\alpha_c = 505 \text{ s}^{-1}$ and $K = 32.3 \text{ mm/As}$). Four different damping values (α_{obj}) are examined:

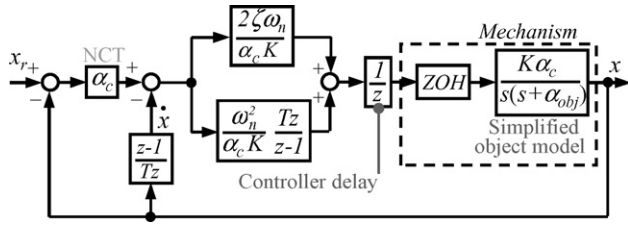


Fig. 17. Sampled-data system used to evaluate the design procedure when α_{obj} changes.

- $\alpha_{obj,1} = 0.001 \text{ s}^{-1}$ (approximately a pure inertia mechanism)
- $\alpha_{obj,2} = 250 \text{ s}^{-1}$
- $\alpha_{obj,3} = 505 \text{ s}^{-1}$
- $\alpha_{obj,4} = 750 \text{ s}^{-1}$

The NCTF control stability limit is evaluated at points $\omega_n T = 0.02, 0.1, 0.25,$ and 0.4 rad .

The results in Fig. 18 show that the practical stability limit for each damping condition is relatively close to the NCTF control stability limit. The average error of approximation between the practical stability limit and the NCTF control stability is 10%. The difference between these stabilities is caused by the integral element of the NCTF controller, which reduces the ultimate values of ζ . Therefore, it is recommended that a margin of safety (at least 10% in this case) is used so that the NCTF control is designed under the safety area of the practical stability limit.

Fortunately, the NCTF control achieves good positioning characteristics at values much lower than ζ_{prac} . As an example, Fig. 19 shows the simulated results of four control systems designed using the system in Fig. 17. In this figure, an object with $\alpha_{obj,4}$ was used and the value of $\omega_n T$ was fixed at 0.25 rad . Step inputs of $1 \mu\text{m}$ were used. The values of ζ were varied by different margins of safety. It is observed that for a good performance, the margins of safety should be larger than 30%.

In the case of the ballscrew mechanism, Fig. 10 shows that the optimum curve for the design of the controller is 60% lower than ζ_{prac} (smaller values of margin of safety tend to deteriorate the performance). Therefore, as a practical rule, a margin of safety for the design should be at least 30%. This value not only compensates for approximation errors, but also indicates the region where the control performance is acceptable.

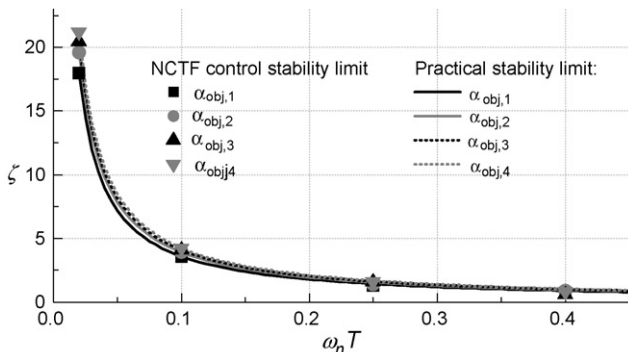


Fig. 18. Practical stability limits under different damping conditions.

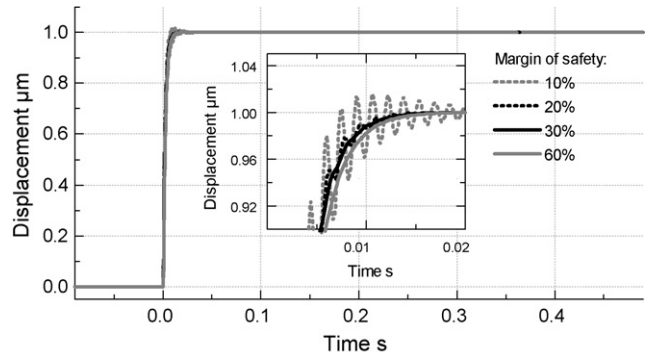


Fig. 19. Effects of the margin of safety on relation to the control performance.

The practical stability limit can be used (considering a margin of safety) for mechanisms with different damping values, even if its variation is large. The result of the condition represented by $\alpha_{obj,1}$ is especially interesting, because it is an indication that ζ_{prac} can be used for friction free mechanisms.

6.2. Case 2: practical stability limit under different Coulomb friction values

In the second case, the nonlinear model of the mechanism in Fig. 2(b) is used for the simulations. The characteristics of the mechanism model are changed by assigning different Coulomb friction values. Variations in Coulomb friction occur often, due to payload variation and lubrication conditions; thus it is important to examine the feasibility of the practical stability limit in such cases. The mechanism model is driven in a closed-loop with the NCTF controller in order to find the practical stability limit and the NCTF control stability limit. Four Coulomb friction values (T_{fmax}) are examined:

- $T_{fmax,1} = 0 \text{ Nm}$
- $T_{fmax,2} = 0.023 \text{ Nm}$
- $T_{fmax,3} = 0.046 \text{ Nm}$ (actual ballscrew mechanism)
- $T_{fmax,4} = 0.138 \text{ Nm}$

The NCTF control stability limit is evaluated at points $\omega_n T = 0.02, 0.05, 0.1, 0.2, 0.3,$ and 0.4 rad for the mechanism with $T_{fmax,3}$, and at points $\omega_n T = 0.02, 0.1, 0.25$ and 0.4 rad for the other cases.

The results in Fig. 20 show the practical stability limit for each friction condition, as well as the markers representing the NCTF control stability. The average error of approximation in this case is 16%. The error of approximation shows that the practical stability limit is useful as an indicator for the choice of compensator gains. Although it does not exactly predict the boundary between the unstable and stable regions, it guarantees that the stable gains are below ζ_{prac} , which greatly helps the designer when selecting the compensator gains. Thus, the practical stability limit is useful as an indicator for the NCTF controller design for mechanisms subjected to large Coulomb friction variations.

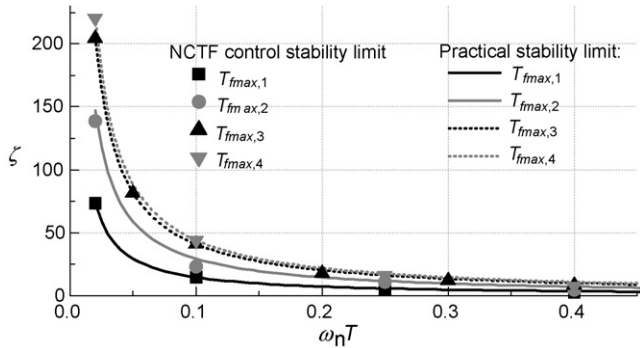


Fig. 20. Practical stability limits under different Coulomb friction.

6.3. Case 3: practical stability limit under different NCT inclinations

In the third case, the inclination of the NCT close to the origin is changed. It is important to consider different inclinations of the NCT because the designer may want to modify the NCT in order to achieve better performance. The procedure used in Section 4 is repeated using the actual mechanism and different NCT inclinations. The practical stability limit (ζ_{prac}) and the NCTF control stability limit are found experimentally and compared. Four NCT's inclinations (α_c) are examined:

$$\begin{aligned} \alpha_{c,1} &= 250 \text{ s}^{-1} \\ \alpha_{c,2} &= 505 \text{ s}^{-1} \text{ (original inclination)} \\ \alpha_{c,3} &= 750 \text{ s}^{-1} \\ \alpha_{c,4} &= 1010 \text{ s}^{-1} \end{aligned}$$

The NCTF control stability limit is evaluated at points $\omega_n T = 0.02, 0.05, 0.1, 0.2, 0.3,$ and 0.4 rad for the controller with $\alpha_{c,2}$, and at points $\omega_n T = 0.02, 0.1, 0.25$ and 0.4 rad for the other cases.

As can be observed from Fig. 21, the practical stability limit curves fit relatively close to the NCTF control stability limit. The approximation error in this case is only 6%. These results prove that a practical stability limit is feasible when the NCTF controller is used with different NCT inclinations, thus allowing the designer to modify the NCT, if necessary.

It is important to notice that, for the three cases considered, the NCTF controller design procedure was the same as the one

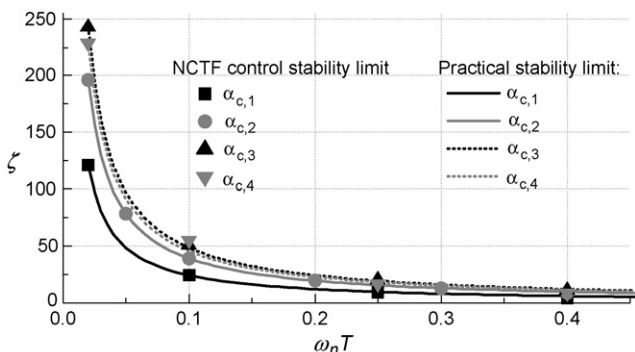


Fig. 21. Practical stability limits using different inclinations of the NCT.

used in Section 4. Therefore, the procedure for the controller parameter determination does not change. The same controller design procedure can be applied when: (1) the damping values change dramatically (including the case in which the mechanism is approximately a pure inertia mechanism), (2) Coulomb friction values vary widely, and (3) different inclinations of the NCT are used.

7. Conclusion

In this study, the NCTF control method was applied to a ballscrew mechanism. The controller was designed without any exact identification of parameters or modeling. The practical stability limit is used to restrict the choice of design parameters ζ and $\omega_n T$ within the stable area. The designed control system achieves a positioning accuracy on the order of nanometers by using large integral values, which also causes an excessive overshoot. This overshoot is reduced by using an antiwindup integrator that is easy to design. PTP positioning performance from 100 nm to 20 mm was evaluated and accuracies better than 10 nm were achieved for all cases. The positioning resolution of the control system is 5 nm even when friction changes. Additional simulations and experiments verified that the NCTF controller design procedure is feasible for three additional cases: (1) when the damping of the mechanism changes, (2) when the Coulomb friction of the mechanism changes, and (3) when the inclination of the NCT changes.

References

- [1] Townsend WT, Kenneth Salisbury J. The effect of coulomb friction and stiction on force control. IEEE Int Conf Robot Automat 1987;4:883–9.
- [2] Armstrong B. Friction: experimental determination, modeling and compensation. In: Proceedings of IEEE international conference on robotics and automation, vol. 3. 1988. p. 1422–7.
- [3] Armstrong-Hélouvy B, DuPont PC, Canudas de Wit, “A survey of models, analysis tools and compensation methods for the control of machines with friction. Automatica 1994;30(7):1083–138.
- [4] Canudas de Wit C, Olsson H, Astrom KJ, Lischinsky P. A new model for control of systems with friction. IEEE Trans Automat Contr 1995;40(3):419–25.
- [5] Ro PI, Hubbel PI. Nonlinear micro-dynamic behavior of a ball-screw driven precision slide system. Precision Eng 1992;14(4):229–36.
- [6] Otsuka J, Masuda T. The influence of nonlinear spring behavior of rolling elements on ultraprecision positioning control systems. Nanotechnology 1998;9:85–92.
- [7] Mao J, Tachikawa H, Shimokohbe A. Precision positioning of a DC-motor-driven aerostatic slide system. Precision Eng 2003;27:32–41.
- [8] Lin TY, Pan YC, Hsieh C. Precision-limit positioning of direct drive systems with the existence of friction. Control Eng Practice 2003;11:233–44.
- [9] Swevers J, Al-Bender F, Ganseman CG, Prajogo T. An integrated friction model structure with improved presliding behavior for accurate friction compensation. IEEE Trans Automat Contr 2000;45(4):675–86.
- [10] Iwasaki M, Shibata T, Matsui N. Disturbance-observer-based nonlinear friction compensation in table drive system. IEEE/ASME Trans Mechatronics 1999;4(1):3–8.
- [11] Ro PI, Shim W, Jeong S. Robust friction compensation for submicrometer positioning and tracking for a ball-screw-driven slide system. Precision Eng 2000;24:160–73.
- [12] Chen CL, Jang MJ, Lin KC. Modeling and high-precision control of a ballscrew driven stage. Precision Eng 2004;28:483–95.

- [13] Otsuka J. Nanometer level positioning using three kinds of lead screws. *Nanotechnology* 1992;3:29–36.
- [14] Otsuka J, Ichikawa S, Masuda T, Suzuki K. Development of a small ultra-precision positioning device with 5 nm resolution. *Measure Sci Technol* 2005;16:2186–92.
- [15] Wahyudi, Sato K, Shimokohbe A. Characteristics of practical control for point-to-point (PTP) positioning systems effect of design parameters and actuator saturation on positioning performance. *Precision Eng* 2003;27:157–69.
- [16] Wahyudi, Albagul A. Performance improvement of practical control method for positioning systems in the presence of actuator saturation. In: *Proceedings of the 2004 IEEE international conference on control applications*. 2004. p. 296–302.
- [17] Sato K. Robust and practical control for PTP positioning. In: *Proceedings of the first international conference on positioning technology*. 2004. p. 394–5.
- [18] Wahyudi, Sato K, Shimokohbe A. Robustness evaluation of new practical control for PTP positioning systems. In: *International conference on advanced intelligent mechatronics proceedings*. 2001. p. 843–8.
- [19] Wahyudi. Robustness evaluation of two control methods for friction compensation of PTP positioning systems. In: *Proceedings of 2003 IEEE conference on control applications*. 2003. p. 1454–8.
- [20] Wahyudi, Sato K, Shimokohbe A. Robustness evaluation of three friction compensation methods for point-to-point (PTP) systems. *Robot Autonomous Syst* 2005;52:247–56.
- [21] Sato K, Nakamoto K, Shimokohbe A. Practical control of precision positioning mechanism with friction. *Precision Eng* 2004;28:426–34.
- [22] Wahyudi, New practical control of PTP positioning systems. PhD Thesis. Tokyo Institute of Technology; 2002.
- [23] Franklin GF, Powell JD, Workman ML. *Digital control of dynamic systems*. 2nd ed. Addison Wesley; 1990.